SUPPLEMENTAL MATERIALS

Supplemental Tables

Supplemental Table S1 (Related to Figure 3). ERG b-wave parameters of scotopic and photopic light responses.

Genotype	**$I_{0.5}$, Scotopic ($cd*s/m^2$)**	**R_{max}, Scotopic (µV)**	**$I_{0.5}$, Photopic ($cd*s/m^2$)**	**R_{max}, Photopic (µV)**
WT	0.0008 ± 0.0006	543 ± 49	0.2 ± 0.1	442 ± 19
α2δ4 KO	0.006 ± 0.0004	221 ± 31	1.33 ± 0.1	136 ± 10
ELFN1 KO	0.005 ± 0.0005	125 ± 5	0.3 ± 0.1	447 ± 17

Supplemental Table S2 (Related to Figure 4). Response Characteristics of Bipolar Cells

Genotype	**WT**			**α2δ4 KO**		
Cell type	ON-RBC	ON-CBC	OFF-CBC	ON-RBC	ON-CBC	OFF-CBC
R_{max}	-150±30 (11)	-61±13 (7)	30±7.9 (5)	NA	-3.1±0.45 (6)	11±1.7(7)
$I_{1/2}$	13±1.0 (11)	14±1.9 (7)	20±1.4 (5)	NA	13±5.3 (6)	13±0.81 (7)

Values of R_{max} are in pA, and for $I_{1/2}$ are in R/rod. Number of cells is indicated as (n)

Supplemental Table S3 (Related to STAR Methods). Primers used for the generation of DNA constructs.

See Suppl Table S3.xlsx file

Supplemental Figures

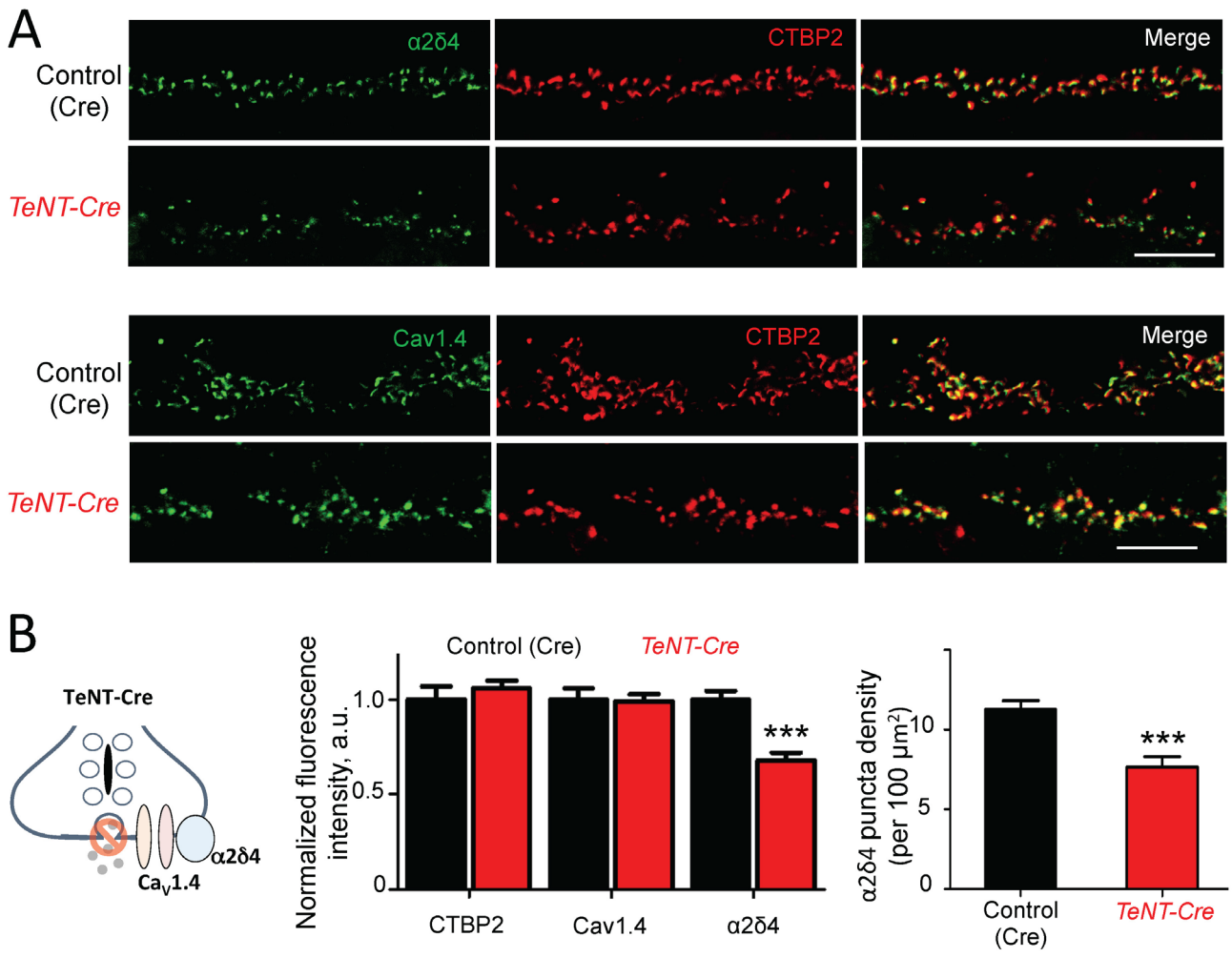

Supplemental Figure S1 (related to Figure 1). Effect of ablating neurotransmitter release in photoreceptors on $Ca_V1.4$ and α2δ4 at the ribbons. A, Immunohistochemical staining for indicated proteins was performed on retinal cross-sections from mice expressing TeNT toxin in photoreceptors by crossing conditional R26-Floxstop mice with the Pchd21-Cre driver line (TeNT-Cre). Littermate mice lacking the TeNT allele but expressing Cre were used as the control. Scale bar, 10 µm. **B**, Scheme illustrating the relationship between the components studied and the effect of TeNT expression on blocking glutamate release from ribbons. Quantification of the observed effects on ribbon morphology (CTBP2) and accumulation of indicated proteins. Two different fields from each retina and two retinas for each genotype were used. ***, $p<0.001$, t-test for α2δ4 puncta density analysis and two-way ANOVA for fluorescence intensity analysis.

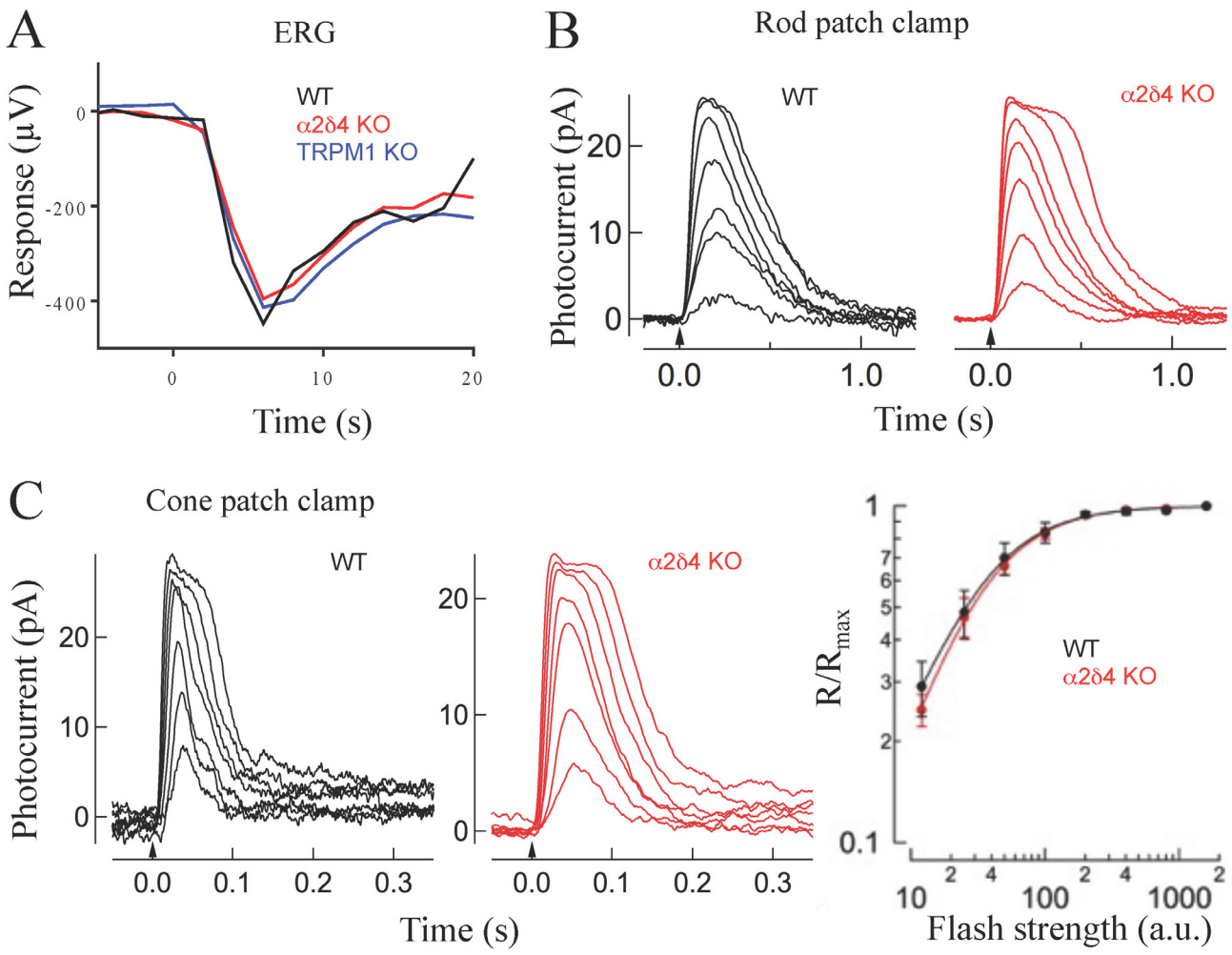

Supplemental Figure S2 (related to Figure 3). Normal rod and cone phototransduction in α2δ4 knockout retinas. A, Representative ERG a-waves in wild-type (black), α2δ4 (red) and TRPM1 (blue) knockout mice. Flash of 100 cd*s/m^2 was delivered to eyes of dark-adapted mice. **B**, Flash families of currents recorded from rods in wild-type (black) and α2δ4 knockout (red) retinas. Flash strengths in both families ranged from 2.4 to 300 photons μm^2. The maximum rod photocurrents did not differ between wild-type and α2δ4 knockouts (16±6.6 pA, n=4 for wild-type; 20±7.1 pA, n=15 for α2δ4; mean±SD, paired t-test p=0.28) **C**, Flash families and response sensitivities of currents recorded from cones in wild-type (black) and α2δ4 knockout (red) retinas. Flash strengths in both families ranged from 600 to 55,000 photons μm^2. The maximum amplitude of cone photocurrents also did not differ between wild-type and α2δ4 knockouts (18±7.9 pA, n=4 for wild-type; 14±4.3 pA, n=6 for α2δ4; mean±SD, paired t-test p=0.67). α2δ4 cones also displayed comparable sensitivity to wild-type cones as shown in the response-intensity relationship (right).

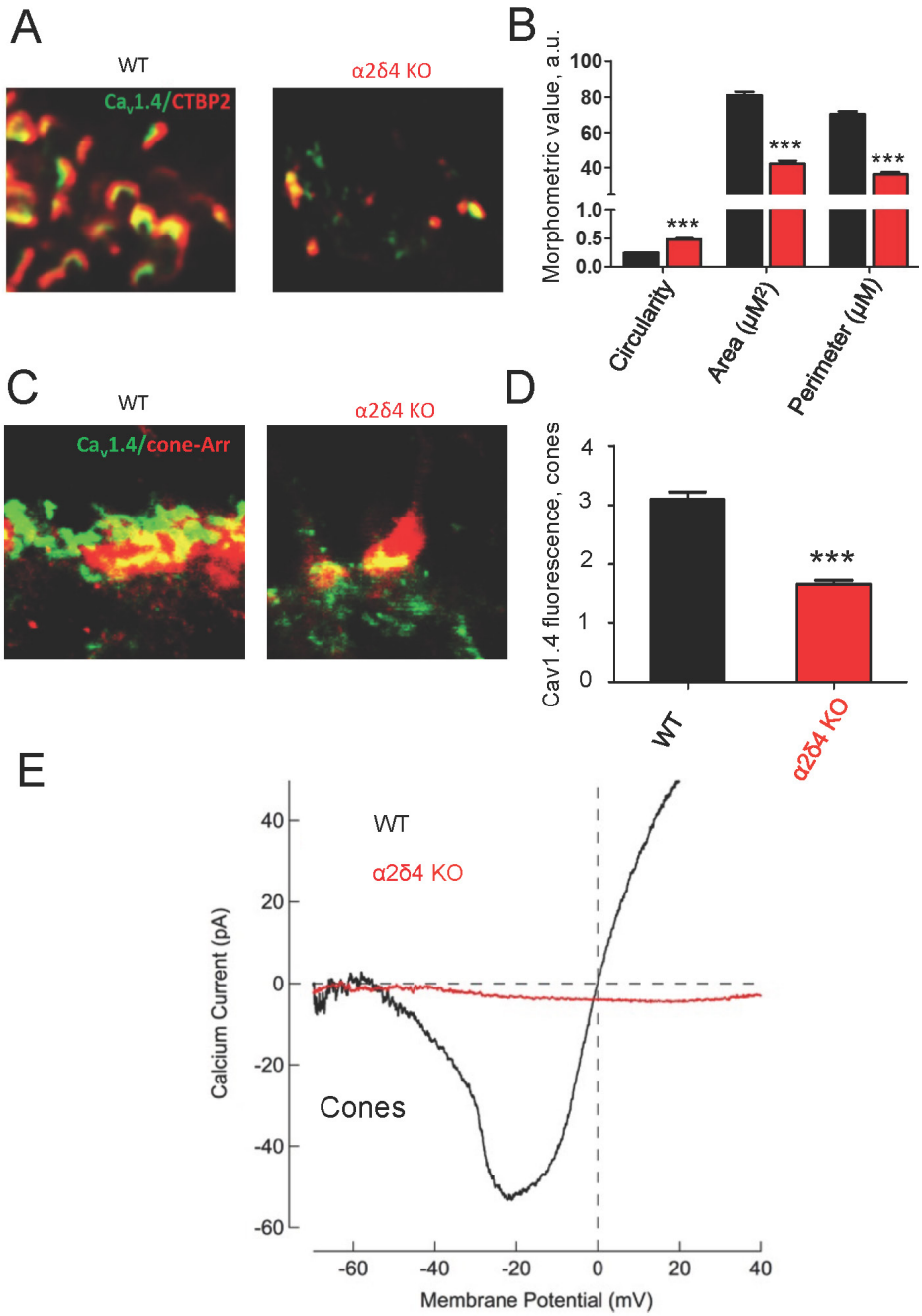

Supplemental Figure S3 (Related to Figure 5). Changes in ribbon synapses associated with α2δ4 loss. A, Immunohistochemical detection of key ribbon components $Ca_V1.4$ and CtBP2 in wild-type (WT) and α2δ4 knockout (α2δ4 KO) retinas. **B**, Quantification of ribbon morphological features. Images from 3 retinas from 3 individual mice for each genotype were analyzed by NIH ImageJ software and the mean values and SEM were potted. ***p<0.01, t-test. Circularity is defined as $4\pi \times [\text{Area}]/[\text{Perimeter}]^2$ with value of 1 indicating perfect circle. As value approaches to 0, it means an increasing elongating shape. **C**, Analysis of $Ca_V1.4$ content in cone pedicles. **D**, Quantification of $Ca_V1.4$ fluorescence intensity in cone pedicles. Images from 3 retinas from 3 individual mice for each genotype were analyzed by Nikon A1 Image analysis software and the mean values and SEM were potted. ***p<0.01, t-test. **E**, Representative $Ca_V1.4$ mediated currents measured from individual cones in retinal slices. Ca^{2+} currents were measured under voltage-clamp while ramping V_m from -80 to +40 mV(Majumder et al., 2013).

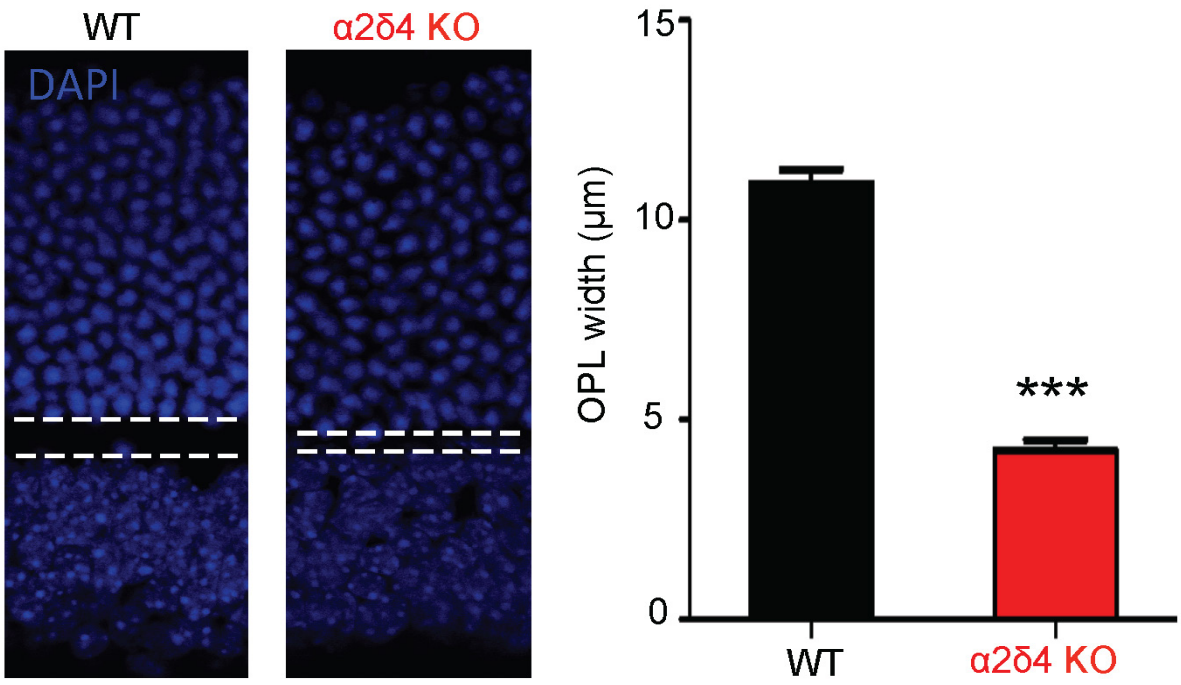

Supplemental Figure S4 (Related to Figure 6). Quantification of the OPL thickness changes in α2δ4 KO retinas. Retinas were stained with DAPI and the OPL was defined as nuclei free zone (no DAPI staining between the outer and inner nuclear layers. Its width was determined in 3 mice of each genotype, mean value and SEM are shown. ***, P<0.001, t-test.

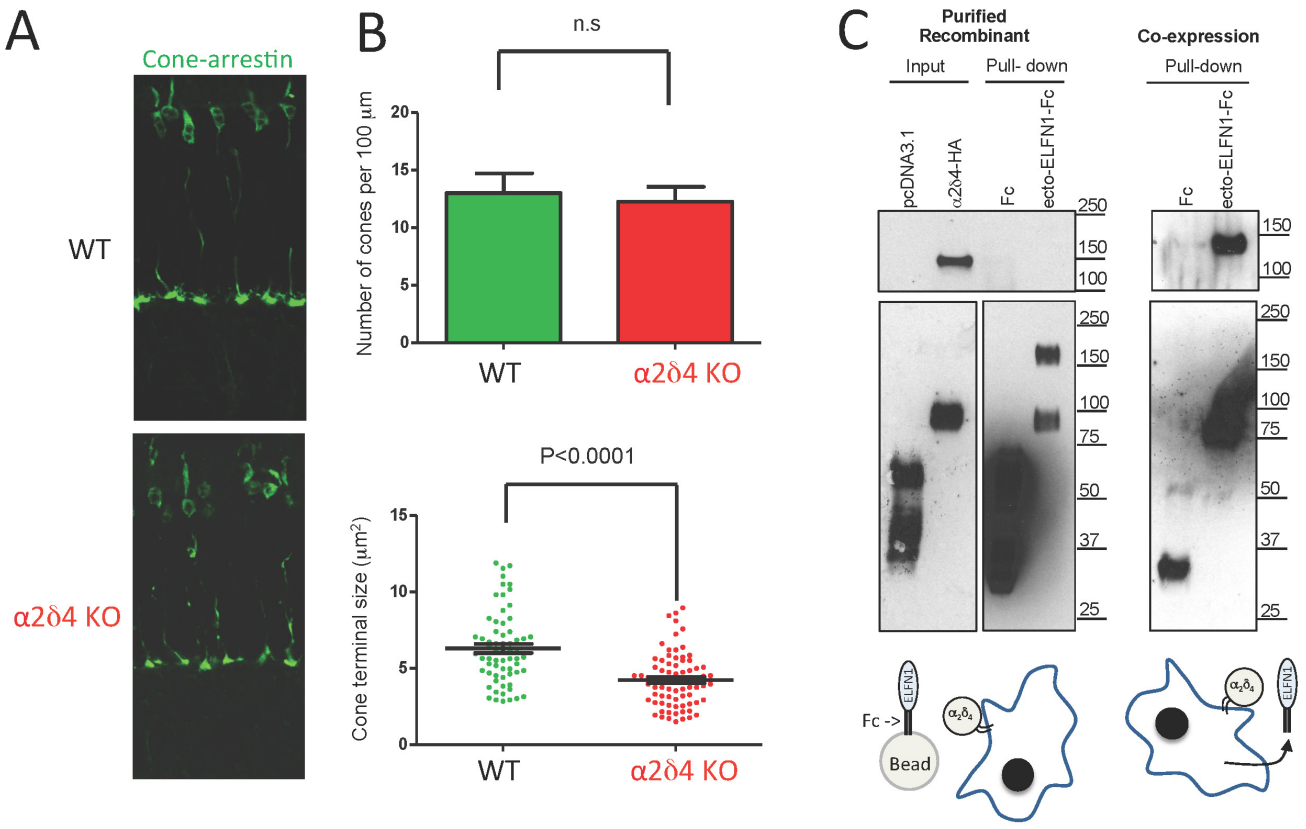

Supplemental Figure S5 (Related to Figure 7). Cellular effects of α2δ4 and its interaction with ELFN1. A, Immunohistochemical detection of cones by cone-arrestin staining in wild-type (WT) and α2δ4 knockout (α2δ4 KO) retinas. **B**, Quantification of cone numbers (upper) and changes in pedicle size (lower). Images from 4 retinas from 3 individual mice for each genotype were analyzed by NIH ImageJ software and the mean values were potted. ***p<0.01, t-test. **C**, Assaying α2δ4 interaction with ELFN1 in reconstituted systems. When purified separately as an Fc-tagged recombinant protein, the ectodomain of ELFN1 fails to pull-down α2δ4 as expressed in HEK293 cells (left). However, when two proteins are co-expressed, they readily form a complex which was detected by the pull-down strategy (right).

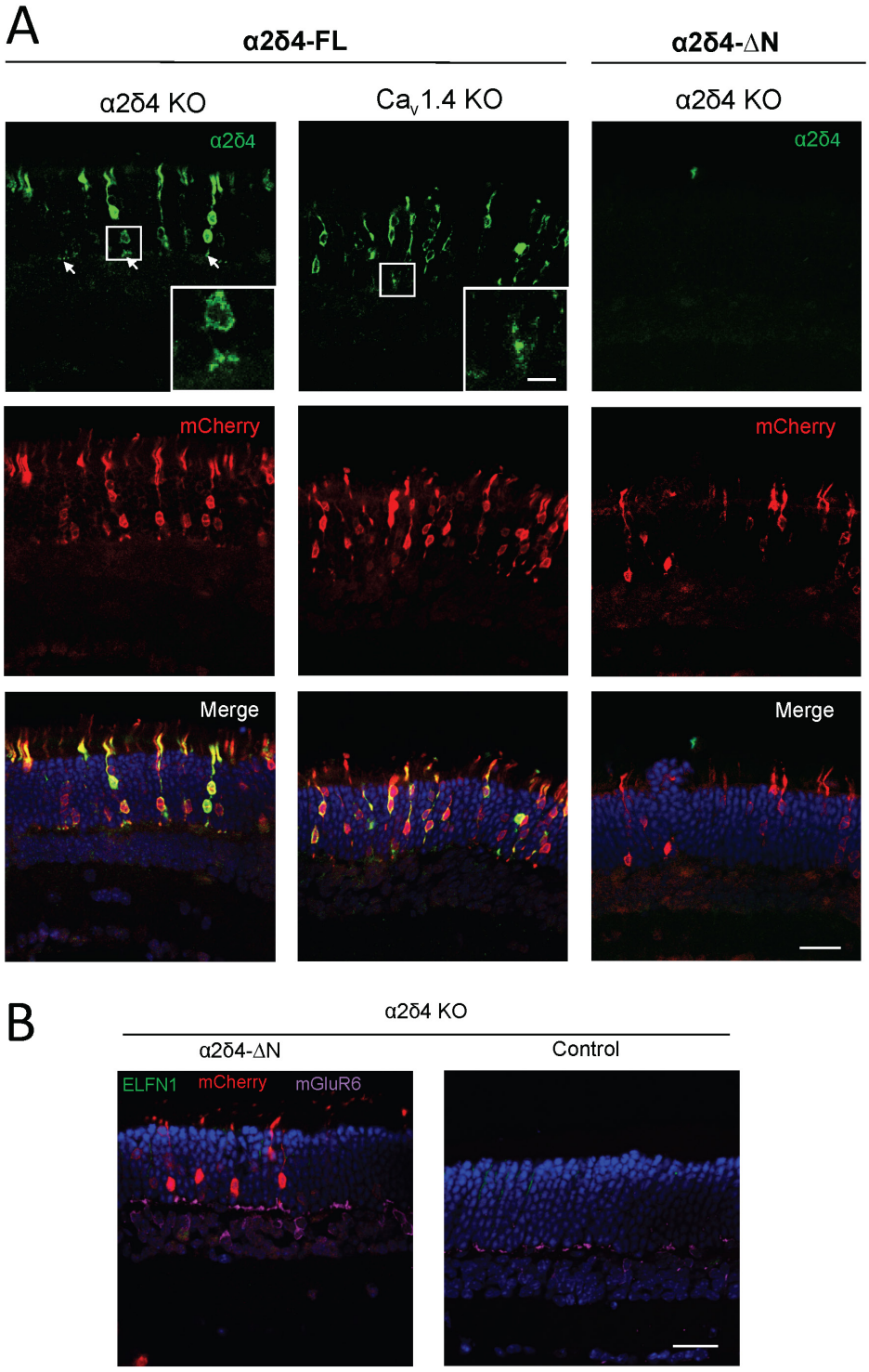

Supplemental Figure S6 (Related to Figure 8). Expression of α2δ4 in rod photoreceptors by *in vivo* electroporation. A, Immunohistochemical detection of α2δ4 constructs expressed in transfected cells of α2δ4 and $Ca_V1.4$ knockout retinas identified by mCherry co-expression. Scale bar: 20 μm. Insert shows α2δ4 content at synaptic terminals. Scale bar: 10 μm. **B**, Expression of the α2δ4 mutant with disrupted N-terminal helices did not rescue the *trans*-synaptic ELFN1-mGluR6 complex. Scale bar: 20 μm.